JACS
JOURNAL OF THE AMERICAN CHEMICAL SOCIETY

ARTICLE

pubs.acs.org/JACS

Roseobacticides: Small Molecule Modulators of an Algal-Bacterial Symbiosis

Mohammad R. Seyedsayamdost,[†] Gavin Carr,[†] Roberto Kolter,[‡] and Jon Clardy*[,†]

[†]Department of Biological Chemistry and Molecular Pharmacology, Harvard Medical School, Boston, Massachusetts 02115, United States

[‡]Department of Microbiology and Molecular Genetics, Harvard Medical School, Boston, Massachusetts 02115, United States

Supporting Information

ABSTRACT: Marine bacteria and microalgae engage in dynamic symbioses mediated by small molecules. A recent study of *Phaeobacter gallaeciensis*, a member of the large roseobacter clade of α-proteobacteria, and *Emiliania huxleyi*, a prominent member of the microphytoplankton found in large algal blooms, revealed that an algal senescence signal produced by *E. huxleyi* elicits the production of novel algaecides, the roseobacticides, from the bacterial symbiont. In this report, the generality of these findings are examined by expanding the number of potential elicitors. This expansion led to the identification of nine new members of the roseobacticide family, rare bacterial troponoids, which provide insights into both their biological roles and their biosynthesis. The qualitative and quantitative changes in the levels of roseobacticides induced by the additional elicitors and the elicitors' varied efficiencies support the concept of host-targeted roseobacticide production. Structures of the new family members arise from variable substituents at the C3 and C7 positions of the roseobacticide core as the diversifying elements and suggest that the roseobacticides result from modifications and combinations of aromatic amino acids. Together these studies support a model in which algal senescence converts a mutualistic bacterial symbiont into an opportunistic parasite of its hosts.

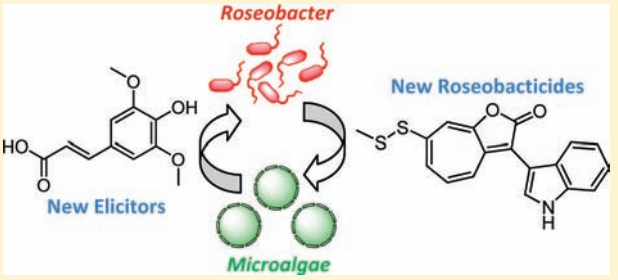

INTRODUCTION

Investigating the chemistry underlying microbial symbioses provides opportunities to discover new small molecules in the context of the biological roles they have evolved to fulfill.[1] In a recent example of this search strategy, we described roseobacticides A and B (Figure 1, **1**, **2**), which contain the previously unreported 1-oxaazulan-2-one core, and their ability to affect marine phytoplankton with nM potency.[2] The bacterial symbiosis partner, or symbiont, that produces these roseobacticides, *Phaeobacter gallaeciensis* BS107,[3] belongs to the roseobacter clade, a large, phylogenetically related group of marine α-proteobacteria that account for up to 25% of all bacteria in typical coastal communities.[4] *P. gallaeciensis* BS107 is easily cultured in the laboratory and under these conditions produces a number of secondary metabolites including the antibiotic tropodithietic acid (**3**), its precursor **4**, and the plant growth promoter phenylacetic acid (**5**).[5−8] *P. gallaeciensis* BS107 associates with *Emiliania huxleyi,* a globally distributed single-celled microalga covered with ornate $CaCO_3$ disks.[2,9] *E. huxleyi* is a major contributor (80−90%) to massive (10^4−10^5 km^2) seasonal algal blooms that are easily visible in satellite images, and it, along with other microphytoplankton, produces nearly half of the Earth's atmospheric oxygen.[10] In addition to fixing CO_2 through photosynthesis, *E. huxleyi* sequesters CO_2 in the $CaCO_3$ disks that surround each algal cell, and also plays a role in the global sulfur cycle by reducing dissolved sulfate to methionine, cysteine, and dimethylsulfoniopropionate (DMSP, **6**).[11] DMSP attracts roseobacter (and other) bacteria, which use it as a carbon and sulfur source.[12] The bacteria can metabolize DMSP to volatile DMS, which in the atmosphere is converted to condensation nuclei for water droplets.[4,13] Thus, roseobacter-microalgal symbioses play key roles in important biogeochemical processes.[4,14]

Numerous studies had shown that the symbioses between bacteria, including those in the roseobacter clade like *P. gallaeciensis* BS107, and microphytoplankton, like *E. huxleyi*, were dynamic; that is, the partners were at times attracted to and at other times repelled by one another.[15,16] It seemed likely that small molecule messages exchanged between the partners elicited these changes in their relationship status. Recent findings by the Harwood and Greenberg laboratories indicated that terrestrial plant-associated bacteria can respond to monomeric components of the heteropolymer lignin that are released into the surrounding soil when plants senesce.[17] As lignin components have been identified in green, red and brown algae, a similar response could plausibly occur in marine plant-bacterial interactions.[18] Examination of *E. huxleyi*, revealed production of significant quantities of *p*-coumaric acid (pCA, **7**), making *E. huxleyi*

Received: August 3, 2011
Published: September 19, 2011

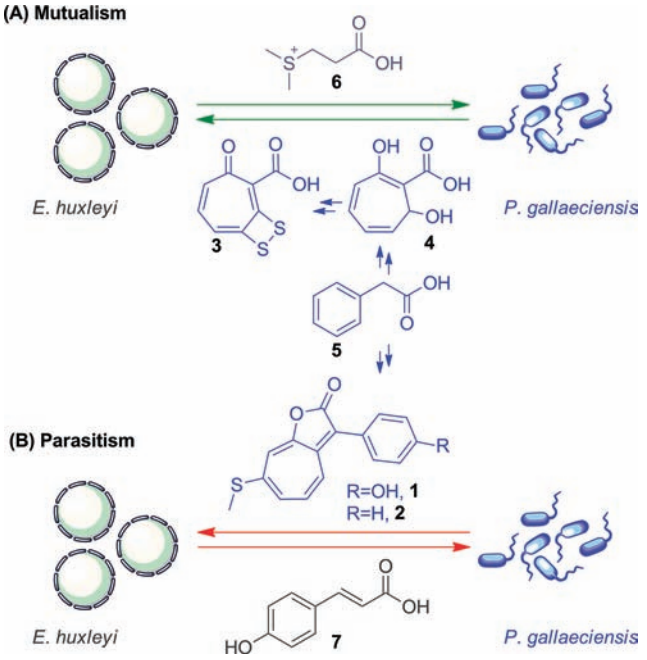

Figure 1. Proposed model for the dynamic interaction between *P. gallaeciensis* B107 and *E. huxleyi*. The two phases of the interaction are shown by green (mutualistic phase) and red (parasitic phase) arrows. Compounds produced by *P. gallaeciensis* BS107 and *E. huxleyi* are shown in blue and gray, respectively. (A) Mutualistic phase of the symbiosis. Under these conditions, the healthy algal host provides DMSP (**6**) and an attachment surface, and the bacterial symbiont provides growth promoter **5** and the antibiotic tropodithietic acid (TDA, **3**), which is biosynthesized from **5** via precursor **4**.[7] (B) Parasitic phase of the symbiosis. When the algal host senesces, it releases pCA (**7**), which elicits the production of antialgal compounds, the roseobacticides (**1**, **2**), likely derived from **5**. Note that **5** is likely a precursor to metabolites that are health-promoting in the mutualistic phase (A) and toxic in the parasitic phase (B). Thus, **5** may be a critical player in the switch from mutualism to parasitism.

the first haptophyte shown to produce lignin components.[2] In addition, our results showed that *P. gallaeciensis* BS107 responds to pCA by producing the roseobacticides, potent algaecides that kill *E. huxleyi*, and affect two other microalgal strains at nM concentrations.

These results, along with previous studies, led to the model shown in Figure 1. In this model, there are two distinct phases in the interaction between *E. huxleyi* and *P. gallaeciensis*: a mutualistic phase, where each partner benefits from the presence of the other, and a parasitic phase, where the bacterial partner converts into a parasite of its host by producing potent antialgal compounds. The interaction is mutualistic when the algal host is healthy. Under these conditions, the host provides the bacteria a solid surface for biofilm formation or attachment along with a C- and S-source (**6**).[19] In return, the bacteria produce antibiotic **3** to protect the host from bacterial pathogens and growth promoter **5** to support algal growth. The relationship changes when the host senesces, which is signaled by the release of pCA by the algal host into the environment. The presence of pCA stimulates the bacteria to produce roseobacticides, which cause cell lysis in *E. huxleyi* with nM potency. This switch from mutualist to parasite allows the bacteria to secure the plentiful food supply provided by the dying host and to associate with healthy algae elsewhere in the bloom. The bacteria's behavioral change corresponds

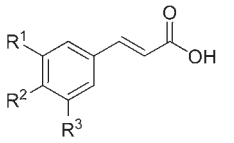

p-coumaric acid (**7**): R^1=R^3=H, R^2=OH
sinapic acid (**8**): R^1=R^3=OCH_3, R^2=OH
ferulic acid (**9**): R^1=OCH_3, R^2=OH, R^3=H
cinnamic acid (**10**): R^1=R^2=R^3=H
caffeic acid (**11**): R^1=R^2=OH, R^3=H

Figure 2. Lignin precursors or breakdown products examined as elicitors of roseobacticide production in this work.

to a metabolic switch since antibiotic **3** is derived from **5** and the core of the roseobacticides can, in principle, be formed by joining the building block of **3** and growth promoter **5**. This switch would transform molecules that facilitate algal growth to potent and selective phytotoxins.[2]

The model in Figure 1 was based on *one* member of the large roseobacter clade, *one* member of the microphytoplankton family, *one* elicitor, and a few bacterial metabolites, and this restricted basis set raises questions about the generality of our model and the small molecules involved. In this report we begin to address some of these questions by examining a larger panel of elicitors, compounds released by the algal host that stimulate production of bacterial secondary metabolites. These studies led to a dramatic expansion of the roseobacticide family through complex quantitative and qualitative changes in bacterial metabolism. We also expand the study to include other members of the roseobacter clade and their responses to the larger panel of elicitors.

MATERIALS AND METHODS

Materials and Strains. Candidate elicitors **7**−**11** (Figure 2) and sea salt used for preparation of culture media were obtained from Sigma-Aldrich. Other media components were from Becton-Dickinson. Roseobacter strains *P. gallaeciensis* BS107 and *P. gallaeciensis* 2.10[15f] were obtained from Prof. Rebecca Case (University of Alberta). Strains *Phaeobacter inhibens* (DSMZ 16374) and *Marinovum algicola* (DSMZ 10251) were obtained from the Deutsche Sammlung von Mikroorganismen and Zellkulturen GmbH (DSMZ).

General Procedures. HPLC purifications were carried out on an Agilent 1200 Series analytical or preparative HPLC system equipped with a photodiode array detector. Low-resolution HPLC-MS analysis was performed on the same analytical system equipped with a 6130 Series ESI mass spectrometer using an analytical Phenomenex Luna C18 column (5 μm, 4.6 × 100 mm) operating at 0.7 mL/min with a gradient of 30% MeCN in H_2O to 100% MeCN over 20 min. High resolution (HR)-HPLC-ESI-MS and HR tandem ESI-MS (HR-MS/MS) were carried out on an Agilent 1200 Series HPLC equipped with a photodiode array detector and a 6520 Series LC/Q-TOF using the same column and gradient as above. HR-MS and HR-MS/MS were calibrated to within 3 ppm and 12 ppm, respectively. ^{1}H, ^{13}C and 2D NMR spectra were recorded in the inverse-detection probe of a Varian Inova spectrometer (600 MHz for ^{1}H, 150 MHz for ^{13}C). Chemical shifts were referenced to the residual solvent peaks in acetone-d_6 or methanol-d_4.

Cultivation of Roseobacter Strains. Preparative-scale (2−8 L) cultivation of *P. gallaeciensis* BS107 (or other roseobacter strains) was carried out in half-strength yeast extract-tryptone-sea salt (YTSS) medium, which consists of (per L): 20 g Sigma sea salt, 2 g yeast extract, and 1.25 g tryptone. *P. gallaeciensis* BS107 (or other roseobacter strains) were streaked out from frozen culture stocks and maintained on Marine Broth

agar plates (Difco 2216) at 30 °C. Overnight cultures were initiated by inoculating 5 mL YTSS medium in 15 mL culture tubes and shaking these overnight at 250 rpm and 30 °C. A 0.5 L Erlenmeyer flask containing 50 mL YTSS medium was inoculated with 0.5 mL of the overnight culture and grown for 12−18 h at 30 °C and 160 rpm. Large 4 L Erlenmeyer flasks, each containing 0.4 L YTSS medium, were inoculated with 4 mL of the overnight culture and supplemented with 1 mM of each of the elicitors (**7**−**11**). The cultures were grown for 3 d at 30 °C and roseobacticides purified as described below.

Elicitor Dose−Response Analysis. Eight to ten 0.25 L Erlenmeyer flasks each containing 25 mL of YTSS medium and a range of elicitor concentrations (between 0 and 1.2 mM) were inoculated with 0.25 mL of an overnight *P. gallaeciensis* BS107 culture prepared as described above. These were grown at 30 °C and 160 rpm. After 3 d, each culture was extracted twice with 25 mL of EtOAc. The organic phase was combined, dried over Na_2SO_4, and subsequently dried in vacuo. The residue was resuspended in 0.3 mL MeOH and analyzed by HPLC-MS as described above. The amount of roseobacticide B (**2**) produced, quantified by mass-ion extraction ($[M + H]^+ = 269$), was plotted against the concentration of the elicitor. The maximal amount of **2** was normalized to 100%, and the EC_{50}, the elicitor concentration where production of **2** was half-maximal, was obtained by fitting the data to eq 1, where B_{max} and B_{min} are the maximal (∼100%) and minimal (∼0%) amounts of **2** and p is a Hill slope parameter to account for variations in the slope.[20] B_{max} and B_{min} were allowed to vary to obtain the optimal fit, carried out by nonlinear least-squares regression analysis.

$$\text{amount of } \mathbf{2} = B_{min} + \frac{B_{max} - B_{min}}{1 + 10^{((EC_{50} - [\text{elicitor}]) \times p)}} \quad (1)$$

Purification of Roseobacticides. After 3 days, the large-scale cultures were extracted twice with an equal volume of EtOAc. The organic phase was combined, dried over Na_2SO_4, and subsequently dried in vacuo. The residue was weighed, resuspended in a small volume of MeOH, mixed with a 3-fold excess of Celite (by weight), and dry-loaded onto a C18-functionalized silica gel column (∼3 g, d = 15 mm, l = 40 mm), which had been equilibrated in 15% MeCN in H_2O. The column was then washed with 10 column volumes (CV) of 15% MeCN, and roseobacticides eluted with a step gradient of 10 CV of 30% MeCN, 10 CV of 75% MeCN, which contained roseobacticides, and 10 CV of 100% MeCN. The 75% MeCN fraction was dried in vacuo and purified on a preparative Phenomenex Phenyl-Hexyl column (5 μm, 21.2 × 250 mm) operating at 12 mL/min with a gradient of 40% MeCN in H_2O to 100% MeCN over 40 min. Fractions that contained roseobacticides, as judged by their UV−visible spectra and by analytical HPLC-MS, were further purified on a semipreparative Agilent Eclipse XDB-C8 column (5 μm, 9.4 × 250 mm) operating at 3 mL/min using a gradient of 35% MeCN in H_2O to 80% MeCN over 40 min. Reapplication of the material onto the same column (or a Supelco Discovery C18 column (10 μm, 10 × 250 mm) or a Phenomenex Luna Phenyl-Hexyl column (5 μm, 10 × 250 mm), depending on the roseobacticide) using the same flow rate and gradient afforded pure material.

Structural Elucidation. Structures of roseobacticides were elucidated using standard 1D (^{1}H and ^{13}C) and 2D (gCOSY, gHSQC, gHMBC, NOESY) NMR spectra. In addition, HR-MS and HR-MS/MS were utilized as described above. ^{1}H NMR spectra, tables of 2D NMR data, HR-MS and HR-MS/MS results for each compound are shown in the Supporting Information. Degradation analysis for **13**−**15**, **19**, and **20** was carried out by incubating a small amount of each compound (∼100 μL, ∼5 μg) with 5 mM (∼10 μL) of the disulfide reducing agent dithiothreitol in MeOH for 1−3 h at room temperature, followed by analysis of the reaction products (∼50 μL) by HPLC-MS as described above.

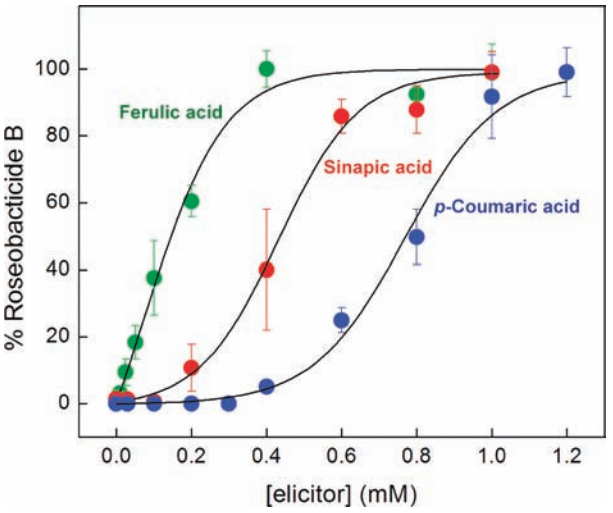

Figure 3. Dose−response analysis for three elicitors of roseobacticide production in *P. gallaeciensis* BS107. The amount of **2** is plotted as a function of the concentrations of pCA (**7**), sinapic acid (**8**), or ferulic acid (**9**), and the data fit to eq 1, yielding an EC_{50} of 0.16 ± 0.02 mM (**9**) and 0.43 ± 0.03 (**8**). The data for **7** are from ref 2, where a value of 0.79 ± 0.03 was determined. For each elicitor, the maximal amount of **2** was normalized to 100%. Each point is the average of two independent measurements; error bars represent standard deviation about the mean.

RESULTS AND DISCUSSION

Additional Roseobacticide Elicitors. In addition to indicating that algal cell wall components may act as elicitors of bacterial metabolite production, our previous results also suggested that *P. gallaeciensis* BS107 is an opportunistic symbiont that could interact with a wide range of hosts. Bioinformatic analyses showed that *E. huxleyi* appears to only contain a pathway for the biosynthesis of H-lignin, the polymer resulting from linkage of pCA units.[2] However, as the nature of lignin components varies with algal hosts,[18b] *P. gallaeciensis* BS107 could also encounter and respond to lignin monomers other than pCA. To test this hypothesis, *P. gallaeciensis* BS107 was incubated with various concentrations of pCA, sinapic acid (**8**) and ferulic acid (**9**), known components of cell wall lignin, as well as with cinnamic acid (**10**) and caffeic acid (**11**), intermediates in the biosynthesis of **7**−**9** (Figure 2),[21] and the level of secondary metabolite production was assessed by HPLC-MS methods. Using **7**, **8**, and **9** as elicitors led to the production of a variety of new metabolites, **10** generated less dramatic results, and **11** produced no observable changes (Supporting Information Figure S1). These results indicate that, in addition to **7**, the lignin precursors **8**−**10** also elicit roseobacticide production in *P. gallaeciensis* BS107 in support of the proposed mutualist-to-parasite switch in our dynamic symbiosis model (Figure 1).

To find optimal conditions for roseobacticide production, a dose-response analysis was carried out with each of the main elicitors. *P. gallaeciensis* BS107 was incubated with varying concentrations of the elicitor, and roseobacticide B production was quantified using HPLC-ESI-MS. The analysis previously indicated a half-maximal effective concentration (EC_{50}) of 0.79 ± 0.03 mM with pCA.[2] With **8** and **9**, we obtained EC_{50} values of 0.43 ± 0.03 and 0.16 ± 0.02 mM, respectively, indicating that these are more potent elicitors of roseobacticide B production in *P. gallaeciensis* BS107 (Figure 3). Each elicitor also shows

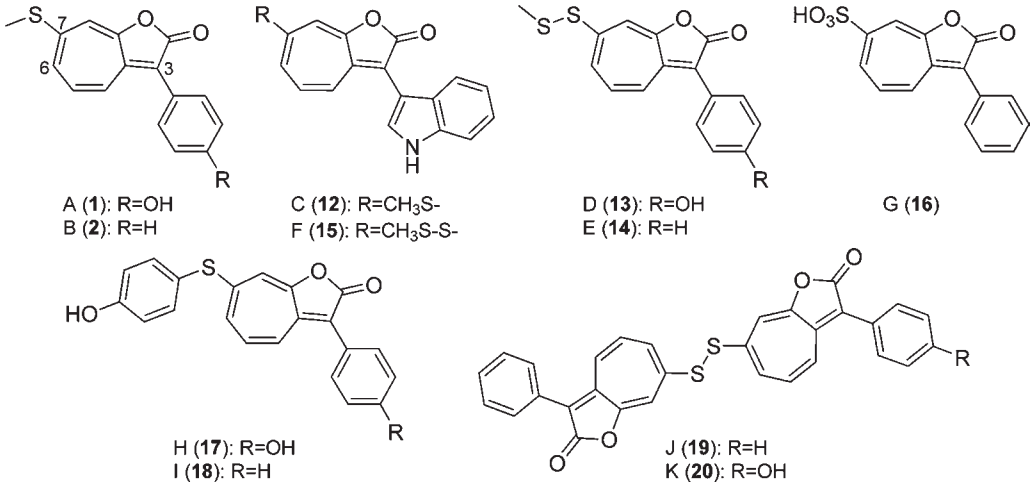

Figure 4. Structures of roseobacticides A−K, of which C−K have been determined in this work. See text for a description.

quantitative changes in the levels of roseobacticide B produced, which may have implications for the interaction of *P. gallaeciensis* BS107 with its algal hosts (see below).

Elucidation of New Roseobacticide Structures. The compounds induced by pCA (**7**), sinapic acid (**8**) and ferulic acid (**9**) were purified from large-scale production cultures of *P. gallaeciensis* BS107 in the presence of each elicitor using standard solid-phase extraction and HPLC methods. The structures were subsequently solved by 1D and 2D NMR spectroscopy, HR-HPLC-ESI-MS and HR-MS/MS. All structures reported below have an H/C ratio < 1, and NMR analysis alone was usually not sufficient for structural elucidation necessitating HR-MS/MS and chemical degradation analyses. Using these techniques, we were able to elucidate the structures of nine new roseobacticides, which fall into four classes (Figure 4): (1) A phenol family with compounds **1**, **13**, and **17**, which contain a thiomethyl, a methyl persulfide, or a *p*-hydroxybenzenethiol moiety at C7 and a phenol group at C3; (2) A phenyl family with compounds **2**, **14**, **16**, and **18** containing a thiomethyl, a methyl persulfide, a sulfonate, or a *p*-hydroxybenzenethiol at C7 and a phenyl group at C3; (3) An indole family with roseobacticides C (**12**) and F (**15**), which contain a thiomethyl or a methyl persulfide at C7, and an indole at C3; and (4) A dimer family with roseobacticides J (**19**) and K (**20**), which consist of two roseobacticides joined through a disulfide linkage.

The structure of the first indole analog, roseobacticide C (Figure 4), was solved readily from 1D and 2D NMR spectra and HR-ESI-MS (Supporting Information Tables S1 and S2). The ^{1}H NMR spectrum revealed a pattern diagnostic of the 1-oxaazulan-2-one core with a different substituent at C3 (Supporting Information Figure S2). ^{1}H NMR, COSY, HSQC, and HMBC spectra (Supporting Information Figure S2 and Table S3) indicated an indole group in agreement with a molecular formula of $C_{18}H_{13}NO_2S$ ($[M + H]^+$ calcd 308.0745, exp 308.0738). HR-MS/MS analysis was consistent with this assignment (Supporting Information Table S2). As with **1** and **2**, the NOESY spectrum of **12** revealed a cross peak between the methyl protons and the proton at C6 (Supporting Information Figure S2). The nature of the substituent at C3 in **1**, **2**, and **12**, points to aromatic amino acids as precursors in roseobacticide biosynthesis. In addition, the presence of indole at the C3 position implicates indoleacetic acid as an intermediate in the biosynthesis of **12**.[2] Because indoleacetic acid is a prominent plant and algal growth promoter,[22] the presence of **12** further supports our model in which the mutualist-to-parasite switch results in a conversion of growth-promoting metabolites into phytotoxins. This finding further highlights the dynamic nature of the algal−bacterial symbiosis (Figure 1).

Scheme 1. Products of the Reactions of 14, 19, and 20 with the Disulfide Reducing Agent Dithiothreitol (DTT)

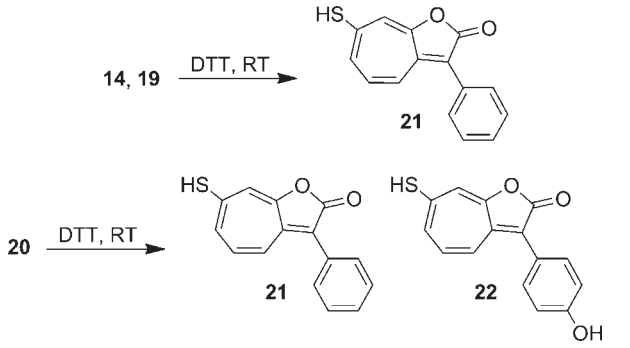

HR-ESI-MS analysis of roseobacticides D, E, and F indicated that they contain an additional sulfur atom relative to roseobacticides A, B, and C, respectively (Supporting Information Table S1). On the basis of the ^{13}C chemical shifts of the methyl groups in **13**−**15**, (22−23 ppm, Supporting Information Figures S3−S5, Tables S4−S6) compared to that of the methyl groups in **1**, **2**, and **12** (~15 ppm, Supporting Information Table S3 and ref 2), we suspected that the former contained a methyl persulfide rather than a thiomethyl group at C7. Incubation of **14** with the reducing agent dithiothreitol (DTT) followed by low-resolution HPLC-MS analysis gave a fragment consistent with loss of methanethiol (Supporting Information Figure S6 and Scheme 1, **21**, $[M + H]^+$ calcd 255.1, exp 255.1) in agreement with a methyl persulfide functionality. In addition, HR-MS/MS analysis with **14** (Figure 5) gave fragments resulting from the loss of a methyl group ($[M + H]^+$ calcd 286.0117, exp 286.0163), loss of a thiomethyl group ($M + H]^+$ calcd 254.0396, exp 254.0436) and loss of a methyl persulfide ($[M + H]^+$ calcd 222.0675, exp 222.0699) establishing the structure of **14** as shown in Figure 4. The corresponding fragments were also obtained with **13** and **15** (Figure 5 and Supporting Information Table S2). The NOESY spectra of **13**−**15** did not reveal a cross peak between the methyl protons and the C6-proton

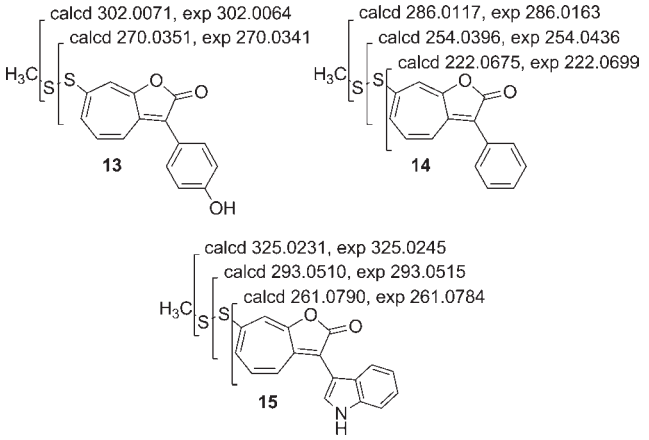

Figure 5. Major $[M + H]^+$ MS/MS fragments obtained with **13**−**15**.

(Supporting Information Figure S7), in agreement with the increased distance in a methyl persulfide substituent, and with the assigned structures.

The ^{1}H NMR and HSQC spectra of **16** revealed a pattern similar to that of **2**, but with major differences in ^{1}H and ^{13}C chemical shifts (Supporting Information Figure S8 and Table S7). The nature of these shifts and the broad peak of this compound during chromatography, even in the presence of 0.1% formic acid, suggested an acidic functionality. HR-MS yielded a formula of $C_{15}H_{10}O_5S$ in line with the presence of a sulfonic acid at C7. HR-MS/MS gave fragments consistent with the loss of SO_2, which is diagnostic for aromatic sulfonates,[23] as well as with the loss of SO_3H and CO (Supporting Information Table S2). The loss of CO occurred in MS/MS spectra of nearly all roseobacticides and presumably originates from collision-induced dissociation of CO from the lactone group. These fragments and the NMR spectra are consistent with the assignment of **16** as a C7-sulfonate-bearing variant of **2**. The incorporation of a sulfonate in place of a thiomethyl group is further demonstration of the ability of roseobacter to modify the oxidation state of sulfur-containing compounds.[4,7,24]

^{1}H NMR, COSY, and HSQC spectra of **17** and **18** were in line with the presence of the 1-oxaazulan-2-one core with the thiomethyl group at C7 replaced with a different substituent. The NMR data (Supporting Information Figures S9−10 and Tables S8−S9) pointed to a phenol-containing moiety at C7. HR-ESI-MS gave molecular formulas of $C_{21}H_{14}O_4S$ and $C_{21}H_{14}O_3S$ for **17** and **18**, respectively, and together with the NMR data were indicative of a bridging sulfur atom and a hydroxyl group in the *para* position, rather than an ether linkage and a free thiol, allowing us to propose that the substituent was a *p*-hydroxybenzenethiol in both cases (Figure 4). This was confirmed by HR-MS/MS, which for both compounds gave the *p*-hydroxybenzenethiol fragment (Table S2, $[M-H]^-$ calcd 123.9983, exp 123.9989 for **17** and exp 123.9987 for **18**), as well as the fragment resulting from loss of the substituent at C7 (**17** $[M + H]^+$ calcd 238.0630, exp 238.0621; **18** $[M + H]^+$ calcd 222.0682, exp 222.0673).

Finally, we were intrigued by **19**, which by HR-MS analysis and ^{1}H NMR, HSQC, and NOESY spectra appeared to be comprised of two roseobacticide B fragments joined end-to-end via a disulfide bond (Supporting Information Figure S11 and Table S10). Treatment of **19** with DTT gave rise to **21**, which was also obtained after treatment of **14** with DTT (Scheme 1 and Supporting Information Figure S6, $[M + H]^+$ calcd 255.1, exp 255.1).

Table 1. Amount of Roseobacticides (mg/L) Produced by *P. gallaeciensis* BS107 and 2.10 as a Function of Elicitor

Roseobacticides	7	8	9	10
		BS107[a]		
A	0.29	0.08	0.2	0.04
B	0.11	1.1	0.5	0.2
C	0.29	0.45	0.25	
D	0.1	0.09		
E	0.18	0.47	0.2	
F	0.15	0.19		
G	*b*	0.13		
H	0.2	0.12		
I	0.06			
J	0.06	0.15	0.1	
K		0.012[c]		
		2.10[d]		
A	0.04	*b*		
B	0.08	0.21	0.7	0.26
H	0.1			0.08
I	0.06		0.17	0.16

[a] Values are averages from three (**7**, **8**) or two (**9**, **10**) independent isolations from large-scale cultures. Standard deviations ranged from 5−40%. [b] Denotes amounts below 0.04 mg/L. [c] An estimate from HPLC-MS comparisons with **19**. [d] Values are averages from two independent experiments from small-scale cultures and comparison with known amounts of roseobacticides. Note that, unlike the data for *P. gallaeciensis* BS107, these are not isolation yields. Standard deviations ranged from 10−35%.

HPLC-HR-MS monitoring of this reaction corroborated the assignment of the new peak as **21** ($[M + H]^+$ calcd 255.0480, exp 255.0483). HR-MS/MS analysis confirmed the structure of **19** revealing a major fragment arising from cleavage of the disulfide bond (Supporting Information Table S2, $[M + H]^+$ calcd 254.0402, exp 254.0398), in line with the molecular formula of $C_{30}H_{18}O_4S_2$ ($[M + H]^+$ calcd 507.0725, exp 507.0736). During purification of **19**, we also observed a faster-migrating fraction with a similar UV−visible spectrum. The molecular formula of $C_{30}H_{18}O_5S_2$ is consistent with **20**, as are the two main fragments observed by HR-MS/MS, which originate from cleavage of the disulfide bond (Supporting Information Table S2, $[M + H]^+$ calcd 270.0351, exp 270.0383 and $[M + H]^+$ calcd 254.0402, exp 254.0420). In addition, treatment of **20** with DTT led to its disappearance and formation of new peaks, one consistent with **21** (Supporting Information Figure S12, $[M + H]^+$ calcd 255.0480, exp 255.0490), and another consistent with **22** ($[M + H]^+$ calcd 271.0429, exp 271.0439, see Scheme 1). The structure of **20** has been assigned based on its migratory properties, UV−vis spectrum, HR-MS, and HR-MS/MS. This compound was produced in very small quantities insufficient for NMR analysis. Thus, the structure shown for **20** remains tentative.

Together, elucidation of the additional elicitors and roseobacticides considerably expands the diversity of small molecules that are likely exchanged in the dynamic roseobacter-algal interaction (Figure 1).

Host-Targeted Roseobacticide Production. Having characterized the structures of the new roseobacticides, we examined the elicitor-dependent differential production of each analog. Table 1 summarizes the amount of each roseobacticide obtained

as a function of elicitors **7**−**10**. While there were batch-to-batch variations, sinapic acid (**8**) was consistently the most effective elicitor with *P. gallaeciensis* BS107 both in the amount and diversity of roseobacticides stimulated followed by pCA (**7**), ferulic acid (**9**), and cinnamic acid (**10**). As lignin monomers vary depending on the algal host,[18b] the quantitative and qualitative changes observed in Table 1 may indicate host-specific production of roseobacticides. These results also indicate that *P. gallaeciensis* BS107 produces a library of roseobacticides, but each in relatively small quantities, perhaps because of the potency of roseobacticide activity, which has been observed with **1** and **2**, and the broad range of hosts with which *P. gallaeciensis* BS107 likely interacts.[2]

Roseobacticide Production by *P. gallaeciensis* 2.10. Because of the ecological contributions of algal−bacterial symbioses, it is important to identify new roseobacticide producers as a measure of the potential environmental significance of this compound class. To assess how widespread roseobacticide production is, and whether the interaction in Figure 1 may be extended to other roseobacter, we examined three of the closest relatives to *P. gallaeciensis* BS107: *Phaeobacter gallaeciensis* 2.10,[15f] isolated from the green macroalga, *Ulva lactuca*; *Phaeobacter inhibens*,[3,25] isolated from the German Wadden Sea; and *Marinovum algicola*,[26] isolated from the dinoflagellate *Prorocentrum lima*. Each strain was grown under identical conditions as *P. gallaeciensis* BS107 in the presence of **7**−**10**. No roseobacticides were observed with *P. inhibens* or *M. algicola* under these conditions. In the case of *P. gallaeciensis* 2.10, various roseobacticides were produced as a function of the elicitor examined (Supporting Information Figure S13); the data are summarized in Table 1. Compound **7** induced the production of **1**, **2**, **17**, and **18**, while **9** stimulated production of large quantities of **2** and **18**. Sinapic acid (**8**) resulted in production of only **2** at approximately similar levels as obtained with **10**. In contrast to *P. gallaeciensis* BS107, **10** was a good elicitor in *P. gallaeciensis* 2.10. Overall, a different trend was observed with *P. gallaeciensis* 2.10 in that **9** was the strongest elicitor, followed by **10**, **7**, and **8**. Production of roseobacticides by *P. gallaeciensis* 2.10 suggests they may be active against macroaglae, or that *P. gallaeciensis* 2.10 is, like its BS107 relative, also an opportunistic algal symbiont. We previously examined *Ruegeria pomeroyi* DSS-3 and *Ruegeria sp.* R11, both of which did not produce roseobacticides.[2] Thus, within the still restricted number of roseobacter members investigated, roseobacticide production appears to be limited to *P. gallaeciensis* strains.

CONCLUSIONS

In this study, we have identified three additional elicitors of roseobacticide production, nine new roseobacticides, and an additional member of the roseobacter clade that also produces these interesting and novel troponoids. The identification of other lignin monomers that lead to roseobacticide production provides support for a model in which algal senescence signals convert a mutualistic interaction into a parasitic one (Figure 1). They also argue that roseobacticide producers are opportunistic algal pathogens that interact with a variety of algal hosts. The structures of the new members of the roseobacticide family provide some insight into their biosynthesis: the substituents at C3 and C7 generate the family's diversity. The nature of the substituents at C3 points to an aromatic amino acid origin in which the three monomeric families originate from phenylalanine, tyrosine, and tryptophan. The diversity and nature of the C7-substituents, coupled with the knowledge that *P. gallaeciensis* BS107 produces dozens of sulfur-, disulfide-, and thiol-containing compounds,[7,24] suggest spontaneous addition of a variety of thiols. These two observations are consistent with a specific pathway for generation of the 1-oxaazulan-2-one core derived from aromatic amino acids, followed by (possibly spontaneous) sulfur-dependent chemistry to provide substituents at the C7 position. Our results also show qualitative and quantitative changes in roseobacticide production depending on the nature of the elicitor in both *P. gallaeciensis* strains. Future biological assays with each roseobacticide variant against a panel of potential algal hosts will elucidate whether the elicitor-dependent changes result from host-targeted roseobacticide production.[27,28] This study has established a large part of the diversity of roseobacticides produced in *P. gallaeciensis* setting the stage for examination of the molecular mechanisms that generate this diversity.

ASSOCIATED CONTENT

Supporting Information. HPLC-ESI-MS analysis of the extracts of *P. gallaeciensis* BS107 and *P. gallaeciensis* 2.10 in the presence of **7**−**11**, 1D/2D NMR spectra, NMR tables, HR-ESI-MS, and HR-MS/MS for **12**−**20**, and degradation analysis of **14**, **19**, and **20**. This material is available free of charge via the Internet at http://pubs.acs.org.

AUTHOR INFORMATION

Corresponding Author
jon_clardy@hms.harvard.edu

ACKNOWLEDGMENT

We thank Rebecca J. Case (University of Alberta) for helpful discussions and for providing strain *P. gallaeciensis* 2.10, and Pierre Stallforth (Harvard Medical School) for the HMBC spectra of **17** and **18** and for helpful comments on the manuscript. This work was supported by the National Institutes of Health (grants AI057159 and GM086258 to J.C., and GM82137 to R.K.). M.R.S. was supported by a postdoctoral fellowship from the Life Sciences Research Foundation (Novartis Fellow) and by an NIH K99 Pathway to Independence Award (Grant 1K99 GM086799-01).

REFERENCES

(1) (a) Piel, J. *Nat. Prod. Rep.* **2009**, *26*, 338. (b) Dudler, R.; Eberl, L. *Curr. Opin. Biotechnol.* **2006**, *17*, 268. (c) Schmidt, E. W. *Nat. Chem. Biol.* **2008**, *4*, 466.

(2) Seyedsayamdost, M. R.; Case, R. J.; Kolter, R.; Clardy, J. *Nat. Chem.* **2011**, *3*, 331.

(3) Martens, T.; Heidorn, T.; Pukall, R.; Simon, M.; Tindall, B. J.; Brinkhoff, T. *Int. J. Syst. Evol. Microbiol.* **2006**, *56*, 1293.

(4) (a) Wagner-Döbler, I.; Biebl, H. *Annu. Rev. Microbiol.* **2006**, *60*, 255. (b) Buchan, A.; Gonzalez, J. M.; Moran, M. A. *Appl. Environ. Microbiol.* **2005**, *71*, 5665.

(5) Brinkhoff, T.; Bach, G.; Heidorn, T.; Liang, L.; Schlingloff, A.; Simon, M. *Appl. Environ. Microbiol.* **2004**, *70*, 2560.

(6) Geng, H.; Belas, R. *J. Bacteriol.* **2010**, *192*, 4377.

(7) Thiel, V.; Brinkhoff, T.; Dickschat, J. S.; Wickel, S.; Grunenberg, J.; Wagner-Döbler, I.; Simon, M.; Schulz, S. *Org. Biomol. Chem.* **2010**, *8*, 234.

(8) Cane, D. E.; Wu, Z.; van Epp, J. E. *J. Am. Chem. Soc.* **1992**, *114*, 8479.

(9) (a) Siegel, D. A.; Franz, B. A. *Nature* **2010**, *466*, 569. (b) Marsh, M. E. *Biochem. Physiol. B Biochem. Mol. Biol.* **2003**, *136*, 743.

(10) (a) Everitt, D. A.; Wright, S. W.; Volkman, J. K; Thomas, D. P.; Lindstrom, E. J. *Deep Sea Res. A* **1990**, *37*, 975. (b) Balch, W. M.; Holligan, P. M.; Ackleson, S. G.; Voss, K. J. *Limnol. Oceanogr.* **1991**, *36*, 629. (c) Holligan, P. M.; Fernandez, E.; Aiken, J.; Balch, W. M.; Boyd, P.; Burkill, P. H.; Finch, M.; Groom, S. B.; Malin, G.; Muller, K.; Purdie, D. A.; Robinson, C.; Trees, C. C.; Turner, S. M.; van der Wal, P. *Global Biogeochem. Cycles* **1993**, *7*, 879.

(11) (a) Wolfe, G. V.; Steinke, M.; Kirst, G. O. *Nature* **1997**, *387*, 894. (b) Wolfe, G. V.; Steinke, M. *Limnol. Oceanogr.* **1996**, *41*, 1151.

(12) (a) Howard, E. C.; Henriksen, J. R.; Buchan, A.; Reisch, C. R.; Bürgmann, H.; Welsh, R.; Ye, W.; Gonzalez, J. M.; Mace, K.; Joye, S. B.; Kiene, R. P.; Whitman, W. B.; Moran, M. A. *Science* **2006**, *314*, 649. (b) Vila-Costa, M.; Simo, R.; Harada, H.; Gasol, J. M.; Slezak, D.; Kiene, R. P. *Science* **2006**, *314*, 652. (c) Seymour, J. R.; Simo, R.; Ahmed, T.; Stocker, R. *Science* **2010**, *329*, 342.

(13) Reisch, C. R.; Stoudemayer, M. J.; Varaljay, V. A.; Amster, I. H.; Moran, M. A.; Whitman, W. B. *Nature* **2011**, *473*, 208.

(14) (a) Charlson, R. J.; Lovelock, J. E.; Andreae, M. O.; Warren, S. G. *Nature* **1987**, *326*, 655. (b) Bates, T. S.; Carlson, R. J.; Gammon, R. H. *Nature* **1987**, *329*, 319.

(15) (a) Miller, T. R.; Belas, R. *Environ. Microbiol.* **2006**, *8*, 1648. (b) Kjelleberg, S.; Steinberg, P.; Givskov, M.; Gram, L.; Manefield, M.; de Nys, R. *Aquat. Microb. Ecol.* **1997**, *13*, 85. (c) Joint, I.; Tait, K.; Callow, M. E.; Callow, J. A.; Milton, D.; Williams, P.; Camara, M. *Science* **2002**, *298*, 1207. (d) Matsuo, Y.; Imagawa, H.; Nishizawa, M.; Shizuri, Y. *Science* **2005**, *307*, 1598. (e) Keshtacher-Liebso, E.; Hadar, Y.; Chen, Y. *Appl. Environ. Microbiol.* **1995**, *61*, 2439. (f) Rao, D.; Webb, J. S.; Holmström, C.; Case, R.; Low, A.; Steinberg, P.; Kjelleberg, S. *Appl. Environ. Microbiol.* **2007**, *73*, 7844. (g) Mayali, X.; Azam, F. *J. Eukaryot. Microbiol.* **2004**, *51*, 139.

(16) Gonzalez, J. M.; Simo, R.; Massana, R.; Covert, J. S.; Casamayor, E. O.; Pedros-Alio, C.; Moran, M. A. *Appl. Environ. Microbiol.* **2000**, *66*, 4237.

(17) Schaefer, A. L.; Greenberg, E. P.; Oliver, C. M.; Oda, Y.; Huang, J. J.; Bittan-Banin, G.; Peres, C. M.; Schmidt, S.; Juhaszova, K.; Sufrin, J. R.; Harwood, C. S. *Nature* **2008**, *454*, 595.

(18) (a) Delwiche, C. F.; Graham, L. E.; Thomson, N. *Science* **1989**, *245*, 399. (b) Martone, P. T.; Estevez, J. M.; Lu, F.; Ruel, K.; Denny, M. W.; Somerville, C.; Ralph, J. *Curr. Biol.* **2009**, *19*, 169. (c) Espineira, J. M.; Novo Uzal, E.; Gomez Ros, L. V.; Carrion, J. S.; Merino, F.; Ros Barcelo, A.; Pomar, F. *Plant Biol.* **2011**, *13*, 59.

(19) Gonzalez, J. M.; Kiene, R. P.; Moran, M. A. *Appl. Environ. Microbiol.* **1999**, *65*, 3810.

(20) Peleg, M.; Normand, M. D.; Damrau, E. *Bull. Math. Biol.* **1997**, *59*, 474.

(21) (a) Davin, L. B.; Jourdes, M.; Patten, A. M.; Kim, K. W.; Vassao, D. G.; Lewis, N. G. *Nat. Prod. Rep.* **2008**, *25*, 1015. (b) Bonawitz, N. D.; Chapple, C. *Annu. Rev. Genet.* **2010**, *44*, 337.

(22) (a) Delker, C.; Raschke, A.; Quint, M. *Planta* **2008**, *227*, 929. (b) Woodward, A. W.; Bartel, B. *Ann. Bot.* **2005**, *95*, 707. (c) Ashen, J. B.; Cohen, J. D.; Goff, L. J. *J. Phycol.* **1999**, *35*, 493.

(23) (a) Eichhorn, P.; Knepper, T. P. *Environ. Toxicol. Chem.* **2002**, *21*, 1. (b) Andreu, V.; Pico, Y. *Anal. Chem.* **2004**, *76*, 2878. (c) Lara-Martin, P. A.; Gomez-Parra, A.; Köchling, T.; Luis Sanz, J.; Mazo-Gonzalez, E. *Environ. Sci. Technol.* **2007**, *41*, 3580.

(24) (a) Dichschat, J. S.; Zell, C.; Brock, N. L. *ChemBioChem* **2010**, *11*, 417. (b) Geng, H.; Bruhn, J. B.; Nielsen, K. F.; Gram, L.; Belas, R. *Appl. Environ. Microbiol.* **2008**, *74*, 1535.

(25) Vandecandelaere, I.; Segaert, E.; Mollica, A.; Faimali, M.; Vandamme, P. *Int. J. Syst. Evol. Microbiol.* **2008**, *58*, 2788.

(26) Lafay, B.; Ruimy, R.; Rausch de Traubenberg, C.; Breittmayer, V.; Gauthier, M. J.; Christen, R. *Int. J. Syst. Bacteriol.* **1995**, *45*, 290.

(27) Ashen, J. B.; Goff, L. J. *Appl. Environ. Microbiol.* **2000**, *66*, 3024.

(28) Comprehensive activity assays of all roseobacticides described herein vs a panel of microalgae is currently in progress.